


Heat fluctuations in chemically active systemsJoël Mabillard ^{1,*}, Christoph A. Weber ^{2,†} and Frank Jülicher ^{3,4,5,‡}¹Max Planck Institute for the Physics of Complex Systems, Nöthnitzer Straße 38, 01187, Dresden, Germany²Faculty of Mathematics, Natural Sciences, and Materials Engineering: Institute of Physics, University of Augsburg, Universitätsstraße 1, 86159 Augsburg, Germany³Max Planck Institute for the Physics of Complex Systems, Nöthnitzer Straße 38, 01187, Dresden, Germany⁴Center for Systems Biology Dresden, Pfotenhauerstrasse 108, 01307 Dresden, Germany⁵Cluster of Excellence Physics of Life, TU Dresden, 01062 Dresden, Germany (Received 14 March 2022; revised 13 June 2022; accepted 14 December 2022; published 13 January 2023)

Chemically active systems such as living cells are maintained out of thermal equilibrium due to chemical events which generate heat and lead to active fluctuations. A key question is to understand on which time and length scales active fluctuations dominate thermal fluctuations. Here, we formulate a stochastic field theory with Poisson white noise to describe the heat fluctuations which are generated by stochastic chemical events and lead to active temperature fluctuations. We find that on large length- and timescales, active fluctuations always dominate thermal fluctuations. However, at intermediate length- and timescales, multiple crossovers exist which highlight the different characteristics of active and thermal fluctuations. Our work provides a framework to characterize fluctuations in active systems and reveals that local equilibrium holds at certain length- and timescales.

DOI: [10.1103/PhysRevE.107.014118](https://doi.org/10.1103/PhysRevE.107.014118)**I. INTRODUCTION**

Active matter systems such as propelled particles [1], molecular motors [2], active gels [3], or active droplets [4] are driven out of thermal equilibrium by chemical processes at molecular scales. In such chemically active systems, a continuous flux of matter and energy drives chemical reactions, generates mechanical forces, or induces motion of molecules and macromolecular compounds. The chemical reactions transduce chemical energy into work or movements, and also release heat into the system. This continuous supply of heat can prevent thermalization to a homogeneous temperature reflecting the nonequilibrium character of active matter.

Living cells are paradigmatic examples of active systems [5–7]. Estimating the temperature inside the cell has been an active field of research over the past few years [8–11]. Active cellular processes such as cell division, cell locomotion, the expression of genes or cellular signaling processes rely on an flux of matter and energy and the availability of chemical fuels such as adenosine triphosphate (ATP) or guanosine triphosphate (GTP) which transduce chemical

energy by hydrolysis to the diphosphate forms ADP and GDP. Such processes produce entropy and maintain the cell away from thermodynamic equilibrium. They also generate and dissipate heat. Under such nonequilibrium conditions, living cells also organize the formation and dissolution of protein-rich condensates. Such condensates are membraneless compartments of distinct chemical composition that play a key role for the spatial organization of cellular biochemistry [12,13]. Recent work studying the formation and dissolution of P granules in *Caenorhabditis elegans* embryos suggests that the formation of these condensates is described by the physics of phase separation [14], which is governed by local thermodynamic equilibrium [15]. It was proposed that local equilibrium conditions hold to a good approximation at length scales of about 100 nm and at microsecond timescales despite the nonequilibrium conditions inside a cell [14]. This raises a fundamental question for chemically active systems in general, namely whether there generally exist length- and timescales for which local equilibrium applies and, if so, what determines the crossover to systems that are lacking locally well-defined thermodynamic fields.

To tackle this question, we consider active and passive heat fluctuations in a chemically active system. The active fluctuations are related to the heat input associated with stochastic chemical reaction events and are described by a stochastic field theory with white noise obeying Poissonian statistics. Poisson white noise has been studied in terms of path probabilities [16–21]. To explore spatiotemporal spectra, we introduce here a generalization of this approach to a field theory in space and time. Passive fluctuations are not related to chemical events but to the stochasticity in the heat transport at local equilibrium. These fluctuations are described

*mabillard@pks.mpg.de

†christoph.weber@physik.uni-augsburg.de

‡julicher@pks.mpg.de

Published by the American Physical Society under the terms of the [Creative Commons Attribution 4.0 International](https://creativecommons.org/licenses/by/4.0/) license. Further distribution of this work must maintain attribution to the author(s) and the published article's title, journal citation, and DOI. Open access publication funded by the Max Planck Society.

by a stochastic field theory with Gaussian white noise [22]. Comparing the magnitudes and the statistical properties of both types of fluctuations, in particular, the correlation function, we identify the temporal and spatial scales at which the local equilibrium hypothesis prevails. Given a characteristic timescale, we derive an analytical expression for the maximal length scale where the passive fluctuations dominate, providing an upper bound for the volume at local equilibrium. The active fluctuations stemming from the chemical reactions could also lead to fluctuations in the concentration fields. In particular, thermophoresis couples heat fluctuations to concentration fluctuations.

The properties of the stochastic field theory with Poisson white noise developed to describe the active fluctuations are investigated. The scaling behavior of the active correlation functions and the characteristics of the noise spectrum are of particular interest due to the Poissonian character of the noise. Although living cells are used throughout this work for illustrative purposes whenever a concrete example is needed, the analysis is more general and applies to other systems where activity is generated by chemical reactions.

This work is organized as follows: in Sec. II we formulate the equations describing the temperature profile inside the active system in three spatial dimensions, define the active and passive fluctuations, and derive their main statistical properties. In Sec. III we discuss the power spectra and higher cumulants of active temperature fluctuations considering systems of spatial dimensions $d = 1, 2, 3$. In Sec. IV, we compare the active and passive temperature correlation obtained in Sec. II and identify the dominant contribution as a function of the time and length scales. We obtain analytical expressions for the scales where active and passive contributions are equal, providing bounds for the time and length scales with active or passive domination. In Sec. V, we estimate the enhancement of the diffusion coefficient due to chemical activity. Our concluding remarks are presented in Sec. VI. An Appendix with more details on derivations is provided at the end of the document.

II. TEMPERATURE FLUCTUATIONS IN CHEMICALLY ACTIVE SYSTEMS

A. Temperature dynamics and fluctuations

In a thermodynamic system, the temperature dynamics follows from the conservation of energy. Temperature dynamics is governed by a balance equation for heat,

$$\rho c_P \partial_t T(\mathbf{x}, t) = -\nabla \cdot \mathbf{j}_q(\mathbf{x}, t) + Q(\mathbf{x}, t), \quad (1)$$

where ρ is the mass density, c_P denotes the specific heat, and \mathbf{j}_q is the heat current density. Moreover, Q is the volumetric heat source, namely the rate of heat released per unit volume due to the conversion, for example, of chemical or mechanical energy into heat q .

We are interested in heat fluctuations due to stochastic chemical events. Individual chemical events give rise to a change in reaction enthalpy h_0 , which is released as heat. With many reactions of the same type taking place at positions x_i

and at times t_i , the heat source is given by

$$Q(\mathbf{x}, t) = h_0 \sum_{i=1}^{n(t, t_0)} \delta^{(3)}(\mathbf{x} - \mathbf{x}_i) \delta(t - t_i), \quad (2)$$

where $n(t, t_0)$ is the number of events having occurred between the initial time t_0 and t . We consider, for simplicity, a Poisson distribution where chemical events occur independently with a probability of a single event at time t and position \mathbf{x} given by $\lambda(\mathbf{x}, t) d^3\mathbf{x} dt$, where λ is the rate per unit volume. The average number of events in the time interval $[t_0, t]$ can thus be expressed as $\langle n(t, t_0) \rangle = \int_V d^3\mathbf{x} \int_{t_0}^t dt' \lambda(\mathbf{x}, t')$, where V is the volume of the system and the angular brackets denote an ensemble average. For a heat release of a single chemical event h_0 , the average rate of energy released per unit volume is $\langle Q(\mathbf{x}, t) \rangle = h_0 \lambda(\mathbf{x}, t)$. The source term Q can be further expressed as

$$Q(\mathbf{x}, t) = h_0 \lambda(\mathbf{x}, t) + \rho c_P \eta_A(\mathbf{x}, t), \quad (3)$$

which defines the space- and time-dependent temperature noise η_A with average $\langle \eta_A(\mathbf{x}, t) \rangle = 0$, which we refer to as active noise. The statistical properties of η_A are discussed in Sec. II B.

The heat current \mathbf{j}_q in Eq. (1) is driven by temperature gradients. In addition, there can be fluctuations that stem from the stochasticity of heat transport, associated with thermal conductivity. The heat current reads

$$\mathbf{j}_q(\mathbf{x}, t) = -\kappa \nabla T(\mathbf{x}, t) + \eta_q(\mathbf{x}, t), \quad (4)$$

where κ is the thermal conductivity. At thermal equilibrium, the noise η_q satisfies

$$\langle \eta_q(\mathbf{x}, t) \rangle = 0, \quad (5a)$$

$$\langle \eta_q^\alpha(\mathbf{x}, t) \eta_q^\beta(\mathbf{x}', t') \rangle = 2k_B T^2 \kappa \delta^{\alpha\beta} \delta^{(3)}(\mathbf{x} - \mathbf{x}') \delta(t - t'), \quad (5b)$$

where the indices α and β denote spatial coordinates and the variance follows from a Green-Kubo relation. Here η_q describes fluctuations of heat transport.

Fluctuations in heat lead to temperature fluctuations which we define and study in the following. Combining Eqs. (3) and (4) leads to an equation for the temperature fluctuations $\delta T \equiv T - \bar{T}$, where \bar{T} denotes the average temperature. To linear order, temperature fluctuations evolve according to

$$\partial_t \delta T(\mathbf{x}, t) = \nabla \cdot (\alpha \nabla \delta T(\mathbf{x}, t)) + \eta_A(\mathbf{x}, t) + \eta_p(\mathbf{x}, t), \quad (6)$$

where $\alpha \equiv \kappa / \rho c_P$ is the thermal diffusivity and $\eta_p \equiv -\nabla \cdot \eta_q / \rho c_P$ is the passive temperature noise. The average temperature \bar{T} satisfies

$$\partial_t \bar{T}(\mathbf{x}, t) = \nabla \cdot (\alpha \nabla \bar{T}(\mathbf{x}, t)) + \frac{h_0}{\rho c_P} \lambda(\mathbf{x}, t). \quad (7)$$

In general, \bar{T} might be time- and space-dependent. For simplicity, we consider here a constant \bar{T} .

The temperature fluctuation profile $\delta T = \delta T_A + \delta T_P$ is the superposition of the two contributions δT_A and δT_P , which stem from the active noise η_A and passive noise η_p , respectively. We consider here active noise that stems from different physical processes than the passive fluctuations, therefore the cross-correlation between active and passive noises vanishes. Using constant α for simplicity, the equations governing the

dynamics of the active or the passive fluctuations $\delta T_{A/P}$ can be written as

$$\partial_t \delta T_{A/P}(\mathbf{x}, t) = \alpha \nabla^2 \delta T_{A/P}(\mathbf{x}, t) + \eta_{A/P}(\mathbf{x}, t). \quad (8)$$

In the remainder of this section, the active and passive fluctuations are investigated separately by determining the corresponding correlation functions $\langle \delta T_A(\mathbf{x}, t) \delta T_A(\mathbf{0}, 0) \rangle$ and $\langle \delta T_P(\mathbf{x}, t) \delta T_P(\mathbf{0}, 0) \rangle$.

B. Active fluctuations

The active fluctuations of temperature $\delta T_A(\mathbf{x}, t)$ are due to active processes and the associated release of energy acting as local sources of heat. Comparing Eq. (2) with Eq. (3), the noise η_A is identified as

$$\eta_A(\mathbf{x}, t) = \frac{h_0}{\rho c_P} \sum_{i=1}^{n(t, t_0)} \delta^{(3)}(\mathbf{x} - \mathbf{x}_i) \delta(t - t_i) - \frac{h_0}{\rho c_P} \lambda(\mathbf{x}, t), \quad (9)$$

which corresponds to a white Poisson noise [16,17,19], characterized by a zero mean and δ -correlated cumulants:

$$\langle \eta_A(\mathbf{x}_1, t_1) \rangle_c = 0, \quad (10a)$$

$$\langle \eta_A(\mathbf{x}_1, t_1) \dots \eta_A(\mathbf{x}_m, t_m) \rangle_c = \left(\frac{h_0}{\rho c_P} \right)^m \lambda(\mathbf{x}_1, t_1) \prod_{i=1}^{m-1} \delta^{(3)}(\mathbf{x}_i - \mathbf{x}_{i+1}) \delta(t_i - t_{i+1}), \quad (10b)$$

where the subscript “c” denotes a cumulant. Note that a Poissonian-type noise with δ -correlated cumulants is ubiquitous in physical chemistry and in biophysical systems [20,21].

For a single chemical event ($n = 1$) corresponding to a heat source occurring at \mathbf{x}' and t' , the heat kernel $G(\mathbf{x}, t | \mathbf{x}', t')$ is the solution of

$$\partial_t G(\mathbf{x}, t | \mathbf{x}', t') = \alpha \nabla^2 G(\mathbf{x}, t | \mathbf{x}', t') + \delta^{(3)}(\mathbf{x} - \mathbf{x}') \delta(t - t'), \quad (11)$$

and is given by [23,24]

$$G(\mathbf{x}, t | \mathbf{x}', t') = \frac{\theta(t - t')}{[4\pi\alpha|t - t'|]^{\frac{3}{2}}} \exp\left[-\frac{(\mathbf{x} - \mathbf{x}')^2}{4\alpha|t - t'|}\right]. \quad (12)$$

Recall that the heat kernel $G(\mathbf{x}, t | \mathbf{x}', t')$ is formally the Green's function of the heat equation and describes the propagation of heat in the system. As the solution of an initial value problem, it breaks time-reversal invariance.

The active temperature fluctuations $\delta T_A(\mathbf{x}, t)$ can be expressed using the heat kernel as

$$\delta T_A(\mathbf{x}, t) = \sum_{i=1}^{n(t, t_0)} \left(\frac{h_0}{\rho c_P} G(\mathbf{x}, t | \mathbf{x}_i, t_i) \right) - \bar{T}(\mathbf{x}, t) \quad (13)$$

and formally corresponds to the field theory of a generalized Poisson noise [18,19]. δT_A describes the fluctuations of the temperature field due to active Poisson-distributed chemical events. Each metabolic event leads to an input of heat, changing the temperature locally, that propagates through the system.

Since the number of chemically active events $n(t, t_0)$ is a fluctuating variable, $\delta T_A(\mathbf{x}, t)$ is a stochastic field. In the following, we study the statistical properties of the active

temperature fluctuations $\delta T_A(\mathbf{x}, t)$. From Eqs. (8) and (10a), the averaged temperature fluctuation vanishes,

$$\langle \delta T_A(\mathbf{x}, t) \rangle = 0, \quad (14)$$

as expected from a white Poisson noise. In Appendix A, we calculate the moment and cumulant generating functionals for δT_A , which give the m -point cumulant ($m > 1$):

$$\begin{aligned} & \langle \delta T_A(\mathbf{x}_1, t_1) \dots \delta T_A(\mathbf{x}_m, t_m) \rangle_c \\ &= \int_{t_0}^t dt' \int_V d^3 \mathbf{x}' \left(\frac{h_0}{\rho c_P} \right)^m \lambda(t', \mathbf{x}') \prod_{i=1}^m G(\mathbf{x}_i, t_i | \mathbf{x}', t'). \end{aligned} \quad (15)$$

Since the heat kernel $G(\mathbf{x}, t | \mathbf{x}', t')$ can be interpreted as a propagator between the points \mathbf{x}' at time t' and \mathbf{x} at time t , the m -point cumulant in Eq. (15) is related to the probability of having all fluctuations $\delta T_A(\mathbf{x}_i, t_i)$ originating from a single event at position \mathbf{x}' and time t' .

Considering for simplicity an infinite size system, a constant rate per unit volume and the long-time limit with $t_1, t_2 \gg t_0$, we find that the second cumulant corresponding to the two-point correlation function is given as

$$\begin{aligned} & \langle \delta T_A(\mathbf{x}_1, t_1) \delta T_A(\mathbf{x}_2, t_2) \rangle_c \\ &= \frac{\lambda h_0^2}{8\pi\alpha\rho^2 c_P^2 |\mathbf{x}_1 - \mathbf{x}_2|} \text{Erf}\left(\frac{|\mathbf{x}_1 - \mathbf{x}_2|}{\sqrt{4\alpha|t_1 - t_2|}}\right). \end{aligned} \quad (16)$$

In the limit $|\mathbf{x}_1 - \mathbf{x}_2| \ll \sqrt{4\alpha|t_1 - t_2|}$, the second cumulant becomes

$$\langle \delta T_A(\mathbf{x}_1, t_1) \delta T_A(\mathbf{x}_2, t_2) \rangle_c \simeq \frac{\lambda h_0^2}{(4\pi\alpha)^{3/2} \rho^2 c_P^2} \frac{1}{\sqrt{|t_1 - t_2|}}, \quad (17)$$

whereas for $\sqrt{4\alpha|t_1 - t_2|} \ll |\mathbf{x}_1 - \mathbf{x}_2|$,

$$\langle \delta T_A(\mathbf{x}_1, t_1) \delta T_A(\mathbf{x}_2, t_2) \rangle_c \simeq \frac{\lambda h_0^2}{8\pi\alpha\rho^2 c_P^2} \frac{1}{|\mathbf{x}_1 - \mathbf{x}_2|}. \quad (18)$$

Note that for equal times $t_1 = t_2$, the relation above is exact.

A key finding of this work is that the two-point correlation function $\langle \delta T_A(\mathbf{x}_1, t_1) \delta T_A(\mathbf{x}_2, t_2) \rangle_c$ of the active fluctuations arising from Poisson-distributed chemical events follows a power-law scaling. This can be interpreted as a critical behavior as there are correlations on all length- and timescales. At a critical point, the equal-time correlation function behaves asymptotically as $1/|\mathbf{x}_1 - \mathbf{x}_2|^{d-2+\eta}$, where d is the dimension of space and η is the critical exponent corresponding to the field anomalous dimension [22]. In three spatial dimensions, $d = 3$, Eq. (18) gives the anomalous dimension $\eta = 0$. These critical fluctuations are a direct consequence of the white Poisson noise and seem to be a characteristic feature of a field theory with stochastic Poisson noise.

C. Passive fluctuations

Even in the absence of active processes, there are fluctuations around the equilibrium temperature [25]. In a system of finite volume, for example, the relaxation toward equilibrium leads to an uncertainty on the actual value of $T(\mathbf{x}, t)$ with respect to the equilibrium temperature of the system. Similarly, in the case of local equilibrium, the temperature is fixed in each volume element with a certain uncertainty.

In addition, the stochasticity of heat transport lead to fluctuations in temperature with an amplitude that depends on the thermal conductivity. These fluctuations enter the heat equation through the Gaussian white noise η_P . Using $\eta_P = -\nabla \cdot \boldsymbol{\eta}_q / (\rho c_P)$ and Eqs. (5), the passive noise satisfies

$$\langle \eta_P(\mathbf{x}, t) \rangle = 0, \quad (19a)$$

$$\langle \eta_P(\mathbf{x}, t) \eta_P(\mathbf{x}', t') \rangle = -\frac{2k_B \bar{T}^2 \alpha}{\rho c_P} \nabla_{\mathbf{x}}^2 \delta^{(3)}(\mathbf{x} - \mathbf{x}') \delta(t - t'). \quad (19b)$$

Now we study the statistics of the passive fluctuations of the temperature δT_P governed by Eq. (8). Due to the Gaussian character of the noise, the only nonvanishing cumulant is the two-point correlation which can be derived using Fourier transformations. Due to the independence of active and passive noise, Eq. (8) in Fourier space becomes

$$-i\omega \delta \tilde{T}_P(\mathbf{q}, \omega) = -\alpha q^2 \delta \tilde{T}_P(\mathbf{q}, \omega) + \tilde{\eta}_P(\mathbf{q}, \omega), \quad (20)$$

when using the definition of the Fourier transform

$$\tilde{f}(\mathbf{q}, \omega) \equiv \int_{t_0}^t dt' \int_V d^3\mathbf{x} f(\mathbf{x}, t') e^{-i(\mathbf{q}\cdot\mathbf{x} - \omega t')}. \quad (21)$$

The passive noise in Fourier space $\tilde{\eta}_P$ satisfies

$$\langle \tilde{\eta}_P(\mathbf{q}, \omega) \rangle = 0, \quad (22a)$$

$$\begin{aligned} \langle \tilde{\eta}_P(\mathbf{q}, \omega) \tilde{\eta}_P(\mathbf{q}', \omega') \rangle \\ = \frac{2k_B \bar{T}^2 \alpha}{\rho c_P} q^2 (2\pi)^4 \delta^{(3)}(\mathbf{q} + \mathbf{q}') \delta(\omega + \omega'). \end{aligned} \quad (22b)$$

The two-point correlation function for passive fluctuations in Fourier space reads [26,27]:

$$\begin{aligned} \langle \delta \tilde{T}_P(\mathbf{q}_1, \omega_1) \delta \tilde{T}_P(\mathbf{q}_2, \omega_2) \rangle_c \\ = \frac{2k_B \bar{T}^2 \alpha}{\rho c_P} q_1^2 \frac{(2\pi)^4 \delta^{(3)}(\mathbf{q}_1 + \mathbf{q}_2) \delta(\omega_1 + \omega_2)}{(\alpha q_1^2 - i\omega_1)(\alpha q_2^2 - i\omega_2)}, \end{aligned} \quad (23)$$

and taking the inverse Fourier transforms gives

$$\begin{aligned} \langle \delta T_P(\mathbf{x}_1, t_1) \delta T_P(\mathbf{x}_2, t_2) \rangle_c \\ = \frac{k_B \bar{T}^2}{\rho c_P (4\alpha\pi |t_1 - t_2|)^{\frac{3}{2}}} \exp\left(-\frac{|\mathbf{x}_1 - \mathbf{x}_2|^2}{4\alpha |t_1 - t_2|}\right). \end{aligned} \quad (24)$$

Contrary to the active fluctuations, the correlation function for the fluctuations around equilibrium does not possess any power-law scaling. In particular, if the time difference $|t - t'|$ is fixed, then the two-point function decays exponentially with the distance $|\mathbf{x} - \mathbf{x}'|$. In the limit $|\mathbf{x}_1 - \mathbf{x}_2| \ll \sqrt{4\alpha |t_1 - t_2|}$, the two-point correlations follow

$$\langle \delta T_P(\mathbf{x}_1, t_1) \delta T_P(\mathbf{x}_2, t_2) \rangle_c \simeq \frac{k_B \bar{T}^2}{\rho c_P} \frac{1}{(4\alpha\pi |t_1 - t_2|)^{\frac{3}{2}}}, \quad (25)$$

whereas for the equal-time correlations, we obtain

$$\langle \delta T_P(\mathbf{x}_1, t) \delta T_P(\mathbf{x}_2, t) \rangle_c = \frac{k_B \bar{T}^2}{\rho c_P} \delta^{(3)}(\mathbf{x}_1 - \mathbf{x}_2). \quad (26)$$

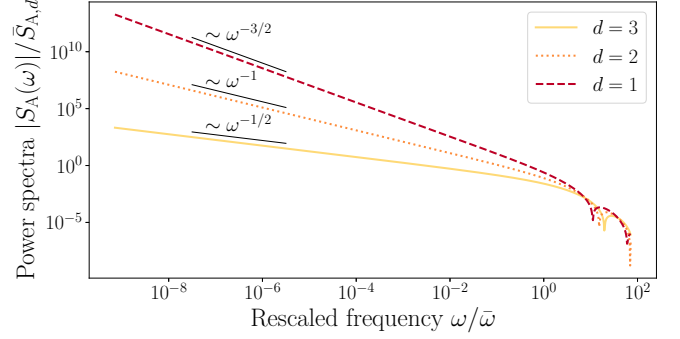


FIG. 1. Power spectra $|S_A|$ defined in Eq. (28) normalized by $\bar{S}_{A,d} \equiv \lambda (\frac{h_0}{\alpha \rho c_P})^2 |\mathbf{x}|^{4-d}$ as function of the rescaled frequency $\omega/\bar{\omega}$ with $\bar{\omega} = \alpha/|\mathbf{x}|^2$ for spatial dimensions $d = 1, 2, 3$. The scaling behavior $\omega^{\frac{d}{2}-2}$ is indicated.

III. POWER SPECTRA AND HIGHER CUMULANTS OF ACTIVE TEMPERATURE FLUCTUATIONS

The formalism developed in Sec. II to describe the active fluctuations is a free Poissonian stochastic field theory with Poisson white noise η_A given by Eq. (9) which has vanishing mean and cumulants given in Eqs. (10a) and (10b). In this section, we discuss key features of the Poisson field theory and highlight differences to a Gaussian stochastic field [22]. For the sake of generality, we consider in this section a d -dimensional space.

The first and the second cumulants are identical to those of Gaussian white noise, but higher-order cumulants, given in Eq. (10b), are nonvanishing and δ -correlated. The latter lead to nontrivial, higher-order cumulants of the field δT_A , which are known exactly in Fourier space as

$$\begin{aligned} \langle \delta \tilde{T}_A(\mathbf{q}_1, \omega_1) \dots \delta \tilde{T}_A(\mathbf{q}_m, \omega_m) \rangle_c \\ = \lambda \left(\frac{h_0}{\rho c_P} \right)^m (2\pi)^{(d+1)} \frac{\delta^{(d)}(\mathbf{q}_1 + \dots + \mathbf{q}_m) \delta(\omega_1 + \dots + \omega_m)}{(\alpha q_1^2 - i\omega_1) \dots (\alpha q_m^2 - i\omega_m)}, \end{aligned} \quad (27)$$

with the Fourier transform defined in Eq. (21). The nonvanishing higher-order cumulants in Eq. (27) demonstrates the non-Gaussian character of the Poisson field theory. We have shown in the previous section that the equal-time correlation function of active temperature fluctuations exhibits as a power-law scaling while for passive fluctuations it is a δ function. To explore this power-law behavior further, we investigate the power spectra of the active temperature fluctuations for systems in 1, 2, and 3 spatial dimensions. We define the spectral density $S_A(|\mathbf{x}|, \omega)$ as follows [28]:

$$\begin{aligned} \langle \delta \hat{T}_A(\mathbf{x}_1, \omega_1) \delta \hat{T}_A(\mathbf{x}_2, \omega_2) \rangle_c \\ = 2\pi S_A(|\mathbf{x}_1 - \mathbf{x}_2|, \omega_1) \delta(\omega_1 + \omega_2), \end{aligned} \quad (28)$$

where $\delta \hat{T}_A(\mathbf{x}, \omega)$ is the Fourier transform of $\delta T_A(\mathbf{x}, t)$ in frequency space. The explicit expressions of the spectral densities are given in Eqs. (B3)–(B5). In the limit of small frequencies, we find that the spectral density scales as $\omega^{\frac{d}{2}-2}$, see Fig. 1 and Eq. (B6). Note that for $d = 2$, we have $S_A \sim \omega^{-1}$ which is a $1/f$ -noise [29–31]. Such type of noise is typical

in biophysical systems [32] and a common feature associated with Poisson shot noise [33].

IV. ACTIVE VERSUS PASSIVE FLUCTUATIONS

We are interested in length- and timescales for which either active or passive fluctuations dominate. To this end, we consider temperature correlation functions which have contributions from passive and active fluctuations. At length scales for which passive fluctuations dominate, local thermodynamics equilibrium is a valid approximation. On the contrary, for length scales where active fluctuations dominate, local equilibrium condition is not satisfied.

The two-point temperature correlation function

$$\mathcal{C}(x, t) = \mathcal{C}_A(x, t) + \mathcal{C}_P(x, t) \quad (29)$$

is the sum of the corresponding correlation functions related to active and passive fluctuations,

$$\mathcal{C}_{A/P}(x, t) \equiv \langle \delta T_{A/P}(\mathbf{x}, t) \delta T_{A/P}(\mathbf{0}, 0) \rangle_c. \quad (30)$$

Note that the correlation function \mathcal{C} is defined here in terms of the cumulants which are identical to the second moments as the mean fluctuations vanish. According to Eqs. (16) and (24), the correlation functions $\mathcal{C}_{A/P}(x, t)$ depend on $x \equiv |\mathbf{x}|$. From the same equations, we find for the two-point temperature correlation function

$$\begin{aligned} \mathcal{C}(x, t) = & \frac{\lambda h_0^2}{8\pi\alpha\rho^2 c_p^2 x} \text{Erf}\left(\frac{x}{\sqrt{4\alpha t}}\right) \\ & + \frac{k_B \bar{T}^2}{\rho c_p (4\alpha\pi t)^{\frac{3}{2}}} \exp\left(-\frac{x^2}{4\alpha t}\right). \end{aligned} \quad (31)$$

The correlation functions $\mathcal{C}_A(x, t)$ and $\mathcal{C}_P(x, t)$ of passive and active fluctuations are shown in Figs. 2(a)–2(f). Figures 2(a)–2(c) depict the active and passive temperature correlations as a function of the length scale x for fixed timescales t . On length scales larger than the diffusion length of passive fluctuations, i.e., $x \gg \sqrt{4\alpha t}$, the passive correlations $\mathcal{C}_P(x, t)$ are exponentially suppressed [Eq. (24)], whereas the active $\mathcal{C}_A(x, t)$ correlations are independent of time t and decrease as a power-law [Eq. (18)]. For $x \ll \sqrt{4\alpha t}$, the active and passive two-point functions, given by Eqs. (17) and (25), respectively, reach finite values. For the timescale

$$\tau = \frac{k_B \bar{T}^2 \rho c_p}{\lambda h_0^2}, \quad (32)$$

these two values are equal, such that $\mathcal{C}_A(0, \tau) = \mathcal{C}_P(0, \tau)$, Fig. 2(b). For timescales larger than τ , the contribution to the correlation function coming from the active fluctuations dominates on all length scales, Fig. 2(c). For timescales smaller than τ , there are length scales where the passive contribution dominates, Fig. 2(a). The scale τ is thus interpreted as the largest timescale for which passive fluctuations can dominate. On timescales smaller than τ , the temperature correlation function in Eq. (31) is dominated by passive fluctuations on small length scales and by active fluctuations on large length scales, Fig. 2(a). We obtain the crossover length, where both

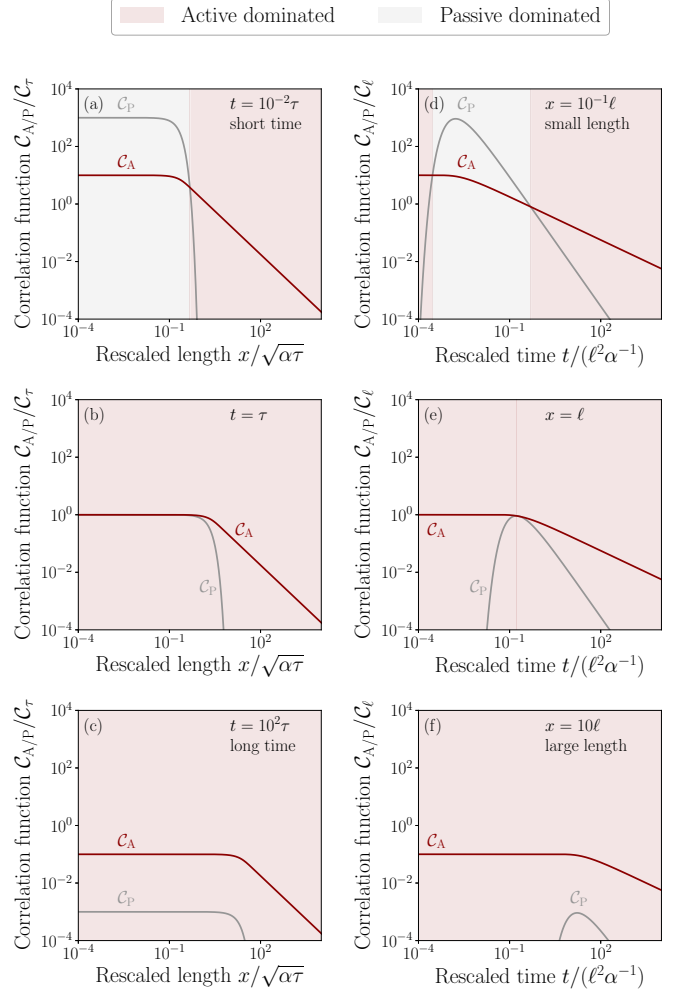


FIG. 2. Normalized two-point correlation functions $\mathcal{C}_P(x, t)$ (gray) and $\mathcal{C}_A(x, t)$ (red) for passive and active fluctuations. (a–c) Temperature correlations $\mathcal{C}_{A/P}$ normalized by \mathcal{C}_τ where $\mathcal{C}_\tau \equiv \mathcal{C}_A(0, \tau) = \mathcal{C}_P(0, \tau)$ with τ given in Eq. (32), as function of normalized distance $x/\sqrt{\alpha\tau}$ for $t = 10^{-2}\tau$ (a), $t = \tau$ (b) and $t = 10^2\tau$ (c). (d–f) Temperature correlation $\mathcal{C}_{A/P}$ normalized by \mathcal{C}_ℓ where $\mathcal{C}_\ell \equiv \mathcal{C}_A(\ell, \ell^2/6\alpha) = \mathcal{C}_P(\ell, \ell^2/6\alpha)$ with ℓ given in Eq. (34), as function of normalized time $t/(\ell^2\alpha^{-1})$ for $x = 10^{-1}\ell$ (d), $x = \ell$ (e), and $x = 10\ell$ (f). The background shade indicates the dominant contribution to the correlation function: active (red), passive (gray). For the vertical line on panel (e), the contributions are equal.

contributions are equal,

$$L_{co}(t) \simeq \left[-2\alpha t W_{-1}\left(-\frac{\pi}{2}(t/\tau)^2\right) \right]^{\frac{1}{2}}, \quad (33)$$

where W_{-1} is the -1 branch of the Lambert W function [34]. To obtain L_{co} , we have used that the active and passive correlations are equal on a length scale that is larger than $\sqrt{4\alpha t}$ and we used Eq. (18) as an approximation for the correlation function \mathcal{C}_A defined in Eq. (30). Note that the length $L_{co}(t)$ exists in a range of timescales t that corresponds to the domain of the Lambert function W_{-1} . For a timescale t smaller than τ , passive fluctuations dominate on length scales smaller than $L_{co}(t)$. Both active and passive correlations are equal for $x =$

$L_{co}(t)$. Active fluctuations dominate the two-point function $\mathcal{C}(x, t)$ for length scales larger than $L_{co}(t)$.

Figures 2(d)–2(f) show the correlation functions $C_P(x, t)$ and $C_A(x, t)$ as function of the timescale t for fixed values of x . On timescales $t \gg x^2/4\alpha$, the active and passive correlations scale in time as $C_A \sim t^{-\frac{1}{2}}$ and $C_P \sim t^{-\frac{3}{2}}$ as shown in Eqs. (17) and (25), respectively. The passive fluctuations have a maximum at $t = x^2/(6\alpha)$, whereas from Eq. (18) the active fluctuations reach their maximal values at $t = 0$. The length scale for which the maximum of $C_P(x, t)$ equals $C_A(x, t)$, Fig. 2(e) (vertical line), is given by

$$\ell = \left[\frac{6^{\frac{3}{2}} \alpha \rho c_P}{\pi^{\frac{1}{2}} e^{\frac{3}{2}} \text{Erf}\left(\sqrt{\frac{3}{2}}\right) k_B \lambda (h_0/k_B \bar{T})^2} \right]^{1/2}, \quad (34)$$

such that $C_A(\ell, \ell^2/6\alpha) = C_P(\ell, \ell^2/6\alpha)$. For length scales larger than ℓ , the contribution to the correlation function coming from the active fluctuations dominates on all timescales, Fig. 2(f). For length scales smaller than ℓ , there exist a range of timescales where the passive contribution is dominant, Fig. 2(d). The scale ℓ is interpreted as the largest length scale for which passive fluctuations can dominate.

On length scales smaller than ℓ , there is an intermediate range of timescales where the dominant contribution to the correlation function stems from passive fluctuations, Fig. 2(d). The upper bound for this range is τ . The lower bound is given by the crossover timescale

$$t_{co}(x) \simeq -\frac{x^2}{6\alpha W_{-1}\left[-e^{-1}\left(\frac{x}{\lambda}\right)^{\frac{4}{3}} \text{Erf}\left(\sqrt{\frac{3}{2}}\right)^{-\frac{2}{3}}\right]}, \quad (35)$$

where W_{-1} is the -1 branch of the Lambert W function. To obtain t_{co} , we have used that the active and passive correlations are equal on a timescale that is smaller than $x^2/4\alpha$ and we used Eq. (18) as an approximation for the correlation function C_A defined in Eq. (30). Note that the time $t_{co}(x)$ exists in a range of length scales x that corresponds to the domain of the Lambert function W_{-1} . For a given length scale x smaller than ℓ , the passive contribution dominates for timescales t in the range $t_{co} < t < \tau$. Finally, we note that $t_{co}(x)$ is the inverse function of $L_{co}(t)$ given in Eq. (33).

The analysis of the active and passive two-point correlations allows us identifying the regions in the temporal and spatial scales in the (t, x) plane which are dominated by either active or passive fluctuations, respectively; see Fig. 3(a). The solid line corresponds to values of x and t for which both contributions are equal. The region dominated by passive fluctuations is bounded by τ of Eq. (32) in the direction of increasing timescale t and by L_{co} of Eq. (33) in the direction of increasing length scale (see dotted line). The largest possible length scale with dominant passive fluctuations is given by ℓ of Eq. (34) and is the maximum of the solid line depicting the boundary between active and passive dominated regions.

On large length or timescales, larger than ℓ and τ , respectively, the system is dominated by active fluctuations. On the contrary, inside the region bounded by L_{co} in the x direction and τ in the t direction, passive fluctuations dominate and equilibrium is a good approximation. To quantify the relative importance of the passive versus the active contribution, we

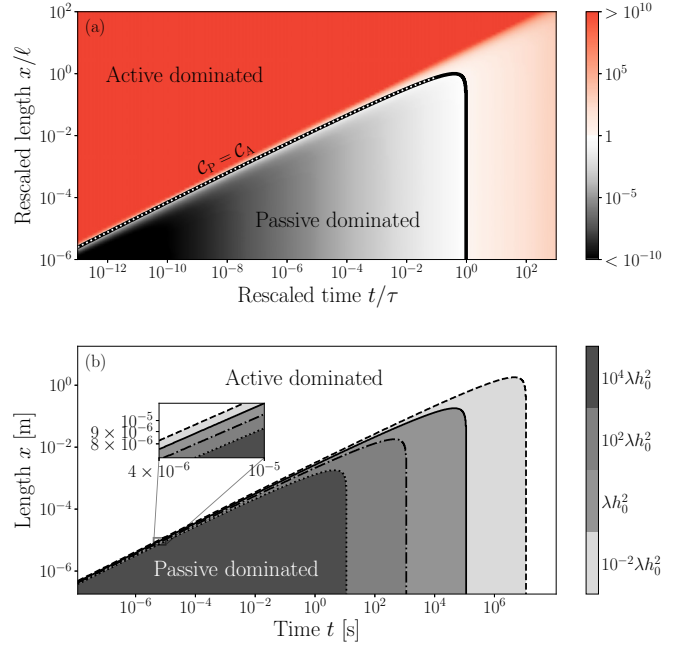


FIG. 3. (a) Active (red) or passive (gray) dominant contribution to the two-point correlation function \mathcal{C} , Eq. (31), in the (t, x) plane as function of the renormalized time and length scales t/τ and x/ℓ with τ given in Eq. (33) and ℓ given in Eq. (34). The solid line depicts the boundary where $C_A = C_P$ between the active and passive dominated regions. The white dots on the solid boundary line indicate the crossover length $L_{co}(t)$ given in Eq. (33). The intensity of the colors describes the ratio C_A/C_P . (b) Regions (shaded, overlaying) where passive fluctuations dominate in the (t, x) plane as a function of timescale t and length scale x . The solid line is the limit between active and passive regions for the parameters values $h_0 = 10k_B \bar{T}$ with $\bar{T} = 289$ K and $\lambda = 2.5 \times 10^4/\text{s}(\mu\text{m})^3$. This can be compared to the corresponding regions when the strength of the noise characterized by λh_0^2 is varied by a factor 10^{-2} (dashed), 10^2 (dot-dashed), or 10^4 (dotted). Note that darker regions partially cover lighter ones. Other parameters are $\alpha = 1.4 \times 10^{-7} \text{ m}^2/\text{s}$, $\rho = 10^3 \text{ kg/m}^3$ and $c_P = 4 \times 10^3 \text{ J}/(\text{kg K})$.

consider the ratio C_A/C_P . In the active region, for timescales smaller than τ and for length scales larger than L_{co} , the passive correlation vanishes exponentially with increasing x and becomes much smaller than the active contribution already for length scales of one order of magnitude larger than L_{co} , as seen in Fig. 3(a). In the passive dominated region, C_P is at least 2, 4, and 6 orders of magnitude larger than C_A for length scales smaller than L_{co} and values of t equal to $\tau/10^2$, $\tau/10^4$, and $\tau/10^6$, respectively. This observation allows identifying the region where the local-equilibrium hypothesis holds, i.e., where the passive correlation function strongly dominates over the active contribution.

For a given chemically active system, our analysis allows us identifying the length- and timescales where local thermodynamic equilibrium is an appropriate description. In the following, we consider the example of biological cells. For the biophysics of P granule assembly and disassembly, it has been suggested that local thermodynamics holds on length scales of 100nm and timescales of tens of nanoseconds [14]. Taking the hydrolysis of ATP as a prototypical chemical event in the cell,

we estimate a reaction enthalpy $h_0 = 10k_B\bar{T}$. Furthermore, we use $\bar{T} = 289\text{K}$ and estimate the rate of events per unit volume as $\lambda \simeq 2.5 \times 10^4/\text{s}(\mu\text{m})^3$, such that the heat production per by unit volume and time is $\langle Q \rangle = 10^3 \text{ W/m}^3$, consistent with estimates for the heat production of living tissues [35,36]. Considering a thermal diffusivity for the cell similar to water $\alpha = 1.4 \times 10^{-7} \text{ m}^2/\text{s}$ [37] and using the mass density $\rho = 10^3 \text{ kg/m}^3$ and the specific heat $c_P = 4 \times 10^3 \text{ J}/(\text{kg K})$ of water, the spatiotemporal scales dominated by passive fluctuations are inside a region, see Fig. 3(b) (gray region bounded by solid line). In particular, the passive region exists for times shorter than $\tau = 1.2 \times 10^5 \text{ s}$ and lengths smaller than $\ell = 0.18 \text{ m}$, respectively. In Ref. [14], it has been observed that 10^{-8} s after a local metabolic event releasing heat h_0 , this heat has spread in a volume of linear dimension of about 10^{-7} m . The corresponding temperature change due to the event is about 10^{-5} K and, thus small. Our analysis shows that for timescales of 10^{-8} s , passive fluctuations dominate up to length scales given by the crossover length $L_{\text{co}}(10^{-8} \text{ s}) = 4.2 \times 10^{-7} \text{ m}$. This demonstrates that our analysis shown in Figs. 3(a) and 3(b) is consistent with estimates given in Ref. [14].

In Fig. 3(a), the ratio between the active and passive correlation functions, C_A/C_P , has been defined as a measure of the chemical activity. The ratio depends linearly on the rate of events per unit volume λ and quadratically on the amount of heat released by individuals events h_0 . Figure 3(b) shows the region of the (t, x) plane dominated by passive fluctuations for different values of $h_0^2\lambda$. Taking the values h_0 and λ estimated above for the living cell as reference (solid line), we observe that increasing (decreasing) λh_0^2 decreases (increases) the area of the passive region. The decrease is mostly due to a decrease of the rightmost boundary along the t direction which can also be seen in Eq. (32) showing that τ is inversely proportional to λh_0^2 . However, the boundary in the x direction does not change significantly when increasing λh_0^2 , as depicted in the inset of Fig. 3(b). The reason for this behavior is that for timescales smaller than τ , passive fluctuations always dominate on the diagonal $x = \sqrt{4\alpha t}$, corresponding to the diffusion length of the passive temperature fluctuations, independently of λ and h_0 . The trend of a decreasing area where passive fluctuations dominate confirms our expectation that the higher the rate and energy released by chemical events, the greater the activity of the system.

V. MOLECULAR DIFFUSION ENHANCED BY ACTIVE FLUCTUATIONS

Considering the diffusion of tracer particles, we discuss how chemical activity could influence the diffusion coefficient. The stochastic motion of a tracer particle with trajectory $\mathbf{X}(t)$ obeys a Langevin equation [38],

$$\frac{d\mathbf{X}(t)}{dt} = D_T \nabla T(\mathbf{X}, t) + \boldsymbol{\eta}_X(t). \quad (36)$$

The noise variance is

$$\langle \eta_X^\alpha(t) \eta_X^\beta(t') \rangle = 2D_0 \delta^{\alpha\beta} \delta(t - t'), \quad (37)$$

where the indices α and β denote spatial coordinates. Here $D_0 = \mu k_B T$ is the passive diffusion coefficient, where μ is the

mobility, and D_T is the thermodiffusion coefficient capturing the Soret effect, with Soret coefficient $S_T \equiv D_T/D_0$.

Temperature fluctuations introduced by chemical activity lead to additional noise on particle motion. This leads to an effective diffusion coefficient $D \equiv D_0 + D_{\text{act}}$, which obeys

$$\langle [\mathbf{X}(t) - \mathbf{X}(0)]^2 \rangle = 6Dt. \quad (38)$$

The effective diffusion coefficient can be obtained from the integral of the velocity auto-correlation function

$$D = \frac{1}{3} \int_0^\infty dt \left\langle \frac{d\mathbf{X}(t)}{dt} \cdot \frac{d\mathbf{X}(0)}{dt} \right\rangle. \quad (39)$$

Using Eqs. (36) and (37), we thus obtain the approximate expression (see Ref. [39] and Appendix C)

$$D_{\text{act}} \simeq \frac{D_T^2}{3V} \int_0^\infty dt \int \frac{d^3\mathbf{q}}{(2\pi)^3} q^2 e^{-Dq^2 t} \times \langle \delta T_A(\mathbf{q}, t) \delta T_A(-\mathbf{q}, 0) \rangle. \quad (40)$$

Using Eq. (16) for the active temperature correlation function, the active contribution to the diffusion coefficient satisfies

$$D_{\text{act}} = \frac{\lambda D_T^2}{6\pi\alpha a} \left(\frac{h_0}{\rho c_P} \right)^2 \frac{1}{(D_0 + D_{\text{act}} + \alpha)}. \quad (41)$$

To estimate the importance of the active fluctuations to diffusion, we consider the ratio D_{act}/D_0 . As shown in Appendix C, we find for this ratio

$$\left(\frac{D_{\text{act}}}{D_0} \right) = -\frac{1}{2} \left(1 + \frac{\alpha}{D_0} \right) + \frac{1}{2} \sqrt{\left(1 + \frac{\alpha}{D_0} \right)^2 + 4C}. \quad (42)$$

Here we have defined the dimensionless coefficient

$$C \equiv \frac{\lambda S_T^2}{6\pi\alpha a} \left(\frac{h_0}{\rho c_P} \right)^2, \quad (43)$$

which depends on the diameter a of the tracer particle and on the Soret coefficient. At equilibrium where the chemical activity $h_0 = 0$, $C = 0$, and $D = D_0$. Active fluctuations become important when $D_{\text{act}} > D_0$. The crossover at $D_{\text{act}} = D_0$ corresponds to $C = C_{\text{co}}$ with

$$C_{\text{co}} \equiv \frac{\alpha}{D_0} + 2. \quad (44)$$

For $C > C_{\text{co}}$, the diffusion coefficient is dominated by the active contribution that enhances diffusion.

Using the parameter values discussed above and motivated by the nonequilibrium conditions in a living cell, we find that the enhanced diffusion of small tracer particles due to chemical activity can be neglected. For example, using the viscosity of water ($\eta = 1.11 \text{ mPa s}$), small particles size a of order 10^{-9} m , and a Soret coefficient $S_T \sim 10^2 \text{ K}^{-1}$ [40], we have $D_{\text{act}}/D_0 \sim \mathcal{O}(10^{-14})$. This estimate supports our findings that local equilibrium can be preserved in the presence of active chemical fluctuations for certain spatiotemporal scales, as discussed above.

VI. DISCUSSION

Our analysis has been motivated by quantitative studies of phase separation in living cells [14]. These raise the

question under what conditions local thermodynamic equilibrium approximations provide an appropriate description of biophysical processes in living cells, even though cells are operating far from thermodynamic equilibrium. Cells host numerous active processes, the paradigmatic example is the activity of many enzymes driven by the hydrolysis of ATP such as the action of molecular motors in the cell. Such activity involves chemical events that release heat and trigger chemical changes of involved biomolecules. Standard approaches to describe such biophysical processes are based on the idea that locally temperature, pressure and other thermodynamic variables are well defined and that the nonequilibrium physics arises at larger scales by a smaller number of degrees of freedom that are maintained away from equilibrium and exhibit nonequilibrium dynamic behaviors. However this raises the question of whether and at which length- and timescales such local equilibrium assumptions hold. Our work shows that even in active systems driven by stochastic active events that release heat, there typically exist length- and timescale regimes where fluctuations are dominated by thermal fluctuations which are consistent with local thermodynamic conditions at a local equilibrium. Therefore in these regimes local equilibrium is an accurate framework to describe the nonequilibrium dynamics that emerges at larger scales. Our analysis is consistent with and completes earlier work where it has been shown that active fluctuations dominate on large spatial or temporal scales [41,42].

To describe nonequilibrium conditions at small scales, we focus our work on fluctuations of heat, which can be either active, i.e., when a chemical event takes place far from equilibrium or passive when they are related to local equilibrium. To characterize active heat fluctuations we have introduced a stochastic Poisson field theory. Because of the Poissonian fluctuations, higher cumulants do not vanish and can be calculated explicitly. Furthermore, we find that correlation functions exhibit power-law behaviors in space and time which correspond to out-of-equilibrium critical behaviors without the need to tune parameters to a critical point. In frequency space, the noise spectrum decreases as a power-law. Notably, in two spatial dimensions, we find $1/f$ -noise. Poisson white noise is usually studied for discrete variables. Here we present a continuum theory in space and time with Poisson statistics.

The approach presented in this work also used some approximations. First, we have considered chemical reactions that are all the same type, and second, we have neglected nonlinearities in the heat equation. While it is straightforward to extend our analysis to include several types of reactions, the problem of nonlinear heat transfer is more challenging and arises already in the absence of activity [24]. For simplicity, we have considered a constant average temperature \bar{T} . In general, the average temperature depends on space and time, for example, when coupled to a thermostat at the boundary, the system reaches a nonequilibrium steady-state, with position-dependent average temperature. A constant average

temperature is a good approximation when studying active fluctuations in a biological cell [14]. All these limitations open new directions for future works. Note that the effect of fluctuations on the diffusion of tracer particles is quite generally weak, also emphasizing that local equilibrium can hold in a broad range of parameters. Our approach can be applied to the diffusion of particles in an active environment, which is different from but related to the problem of the diffusion of active enzymes [43–45].

Our analysis and the results presented here can also be applied to other active systems. Examples are particles propelled by chemical fuel, transport processes that generate heat via stochastic molecular events. The description of fluctuations in such systems in general requires accounting for the coupling to mass or momentum transfer suggesting more complex behaviors of the corresponding correlation functions [1].

We have shown that a field theory with a stochastic Poisson noise provides a framework that is well-suited to describe out-of-equilibrium fluctuations. Moreover, with the inclusion of sinks, such a theory provides a new description for birth and death processes and could potentially be extended to more general reaction-diffusion problems. Another direction to investigate is going beyond the free theory by considering correlations between the metabolic events that generate heat. For the white Poisson noise considered in this work, the Poisson-distributed chemical events have been treated as independent and uncorrelated. Interactions between the events lead to a correlated active noise, corresponding to a colored Poisson noise.

ACKNOWLEDGMENTS

The authors thank Peter Hänggi (University of Augsburg), Uwe Täuber (Virginia Tech), and Pierre Gaspard (Université Libre de Bruxelles) for stimulating discussions and comments on the manuscript.

APPENDIX A: STATISTICS OF ACTIVE FLUCTUATIONS

In this Appendix, we review the statistical properties of the temperature fluctuations δT_A due to the Poisson white noise. For the sake of generality, a system of d spatial dimensions is considered. The temperature fluctuation δT_A given in Eq. (13) is a stochastic field, as it depends on the number of events $n(t, t_0)$ obeying Poisson statistics and the time and location of each metabolic event, whose probability distribution is given by $\lambda(\mathbf{x}, t)d\mathbf{x}dt/\Lambda$ where Λ is the normalization, defined as

$$\Lambda \equiv \int_{t_0}^t dt' \int_V d^d\mathbf{x} \lambda(\mathbf{x}, t'), \quad (\text{A1})$$

which corresponds to the average number of events $\langle n(t, t_0) \rangle$. The moment generating functional for δT_A is defined as

$$\begin{aligned}\Phi_{t,V}[u] &\equiv \left\langle \exp \left[i \int_{t_0}^t dt' \int_V d^d \mathbf{x} u(\mathbf{x}, t') \delta T_A(\mathbf{x}, t') \right] \right\rangle \\ &= \exp \left[-i \int_{t_0}^t dt' \int_V d^d \mathbf{x} u(\mathbf{x}, t') \bar{T}(\mathbf{x}) \right] \left\langle \prod_{i=1}^{n(t,t_0)} \exp \left[i \frac{h_0}{\rho c_P} \int_{t_0}^t dt' \int_V d^d \mathbf{x} u(\mathbf{x}, t') G(\mathbf{x}, t' | \mathbf{x}_i, t_i) \right] \right\rangle.\end{aligned}$$

To evaluate the ensemble average we generalize the method of Ref. [16] to include the spatial dependence of the stochastic variable. An integration over the probability density of the individual events and an average over the Poisson distribution $P(n(t, t_0) = n) = \frac{1}{n!} e^{-\Lambda} \Lambda^n$ are performed. We obtain

$$\begin{aligned}&\left\langle \prod_{i=1}^{n(t,t_0)} \exp \left[i \frac{h_0}{\rho c_P} \int_{t_0}^t dt' \int_V d^d \mathbf{x} u(\mathbf{x}, t') G(\mathbf{x}, t' | \mathbf{x}_i, t_i) \right] \right\rangle \\ &= \sum_{n=0}^{\infty} \frac{1}{n!} e^{-\Lambda} \Lambda^n \prod_{i=1}^n \frac{1}{\Lambda} \int_{t_0}^t dt_i \int_V d^d \mathbf{x}_i \lambda(\mathbf{x}_i, t_i) \exp \left[i \frac{h_0}{\rho c_P} \int_{t_0}^t dt' \int_V d^d \mathbf{x} u(\mathbf{x}, t') G(\mathbf{x}, t' | \mathbf{x}_i, t_i) \right] \\ &= \sum_{n=0}^{\infty} \frac{1}{n!} e^{-\Lambda} \left\{ \int_{t_0}^t dt'' \int_V d^d \mathbf{x}' \lambda(\mathbf{x}', t'') \exp \left[i \frac{h_0}{\rho c_P} \int_{t_0}^t dt' \int_V d^d \mathbf{x} u(\mathbf{x}, t') G(\mathbf{x}, t' | \mathbf{x}', t'') \right] \right\}^n \\ &= \exp \left(- \int_{t_0}^t dt'' \int_V d^d \mathbf{x}' \lambda(\mathbf{x}', t'') \left\{ 1 - \exp \left[i \frac{h_0}{\rho c_P} \int_{t_0}^t dt' \int_V d^d \mathbf{x} u(\mathbf{x}, t') G(\mathbf{x}, t' | \mathbf{x}', t'') \right] \right\} \right).\end{aligned}\quad (\text{A2})$$

The moment generating functional is therefore

$$\Phi_{t,V}[u] = \exp \left(- \int_{t_0}^t dt'' \int_V d^d \mathbf{x}' iu(\mathbf{x}', t'') \bar{T}(\mathbf{x}') + \lambda(\mathbf{x}', t'') \left\{ 1 - \exp \left[i \frac{h_0}{\rho c_P} \int_{t_0}^t dt' \int_V d^d \mathbf{x} u(\mathbf{x}, t') G(\mathbf{x}, t' | \mathbf{x}', t'') \right] \right\} \right).\quad (\text{A3})$$

The cumulant generating functional $\Psi_{t,V}[u] \equiv \ln \Phi_{t,V}[u]$ reads

$$\Psi_{t,V}[u] = \int_{t_0}^t dt'' \int_V d^d \mathbf{x}' \lambda(\mathbf{x}', t'') \left\{ \exp \left[i \frac{h_0}{\rho c_P} \int_{t_0}^t dt' \int_V d^d \mathbf{x} u(\mathbf{x}, t') G(\mathbf{x}, t' | \mathbf{x}', t'') \right] - 1 \right\} - iu(\mathbf{x}', t'') \bar{T}(\mathbf{x}').\quad (\text{A4})$$

The mean value vanishes and the m -point cumulant, for $m > 1$, is

$$\begin{aligned}\langle \delta T_A(\mathbf{x}_1, t_1) \dots \delta T_A(\mathbf{x}_m, t_m) \rangle_c &= (-i)^m \frac{\delta^m}{\delta u(\mathbf{x}_1, t_1) \dots \delta u(\mathbf{x}_m, t_m)} \Psi_{t,V}[u] \Big|_{u=0} \\ &= \left(\frac{h_0}{\rho c_P} \right)^m \int_{t_0}^t dt' \int_V d^d \mathbf{x} \lambda(\mathbf{x}, t') G(\mathbf{x}_1, t_1 | \mathbf{x}, t') \dots G(\mathbf{x}_m, t_m | \mathbf{x}, t'),\end{aligned}\quad (\text{A5})$$

where in d spatial dimension, the heat kernel G reads

$$G(\mathbf{x}, t | \mathbf{x}', t') = \frac{\theta(t - t')}{[4\pi\alpha|t - t'|]^{\frac{d}{2}}} \exp \left[-\frac{(\mathbf{x} - \mathbf{x}')^2}{4\alpha|t - t'|} \right].\quad (\text{A6})$$

Let us also highlight the derivation of the 2-point cumulant for a constant rate per unit volume $\lambda(\mathbf{x}, t) = \lambda$ and sending the limit of spatial integration to infinity. We have

$$\begin{aligned}\langle \delta T_A(\mathbf{x}_1, t_1) \delta T_A(\mathbf{x}_2, t_2) \rangle_c &= \lambda \left(\frac{h_0}{\rho c_P} \right)^2 \int_{t_0}^t dt' \int_{\mathbb{R}^d} d^d \mathbf{x} G(\mathbf{x}_1, t_1 | \mathbf{x}, t') G(\mathbf{x}_2, t_2 | \mathbf{x}, t') \\ &= \frac{\lambda h_0^2}{(4\pi\alpha)^d \rho^2 c_P^2} \int_{t_0}^t dt' \frac{\theta(t_1 - t') \theta(t_2 - t')}{[(t_1 - t')(t_2 - t')]^{\frac{d}{2}}} \exp \left[-\frac{(\mathbf{x}_1 - \mathbf{x}_2)^2}{4\alpha(t_1 + t_2 - 2t')} \right] \\ &\quad \times \int_{\mathbb{R}^d} d^d \mathbf{x} \exp \left\{ -\frac{(t_1 + t_2 - 2t')}{4\alpha(t_1 - t')(t_2 - t')} \left[\mathbf{x} - \frac{(t_2 - t')\mathbf{x}_1 + (t_1 - t')\mathbf{x}_2}{t_1 + t_2 - 2t'} \right]^2 \right\},\end{aligned}\quad (\text{A7})$$

assuming that $\mathbf{x}_1 \neq \mathbf{x}_2$ and $t_1 \neq t_2$ and using that

$$\frac{(\mathbf{x}_1 - \mathbf{x})^2}{t_1 - t'} + \frac{(\mathbf{x}_2 - \mathbf{x})^2}{t_2 - t'} = \frac{(t_1 + t_2 - 2t')}{(t_1 - t')(t_2 - t')} \left(\mathbf{x} - \frac{(t_2 - t')\mathbf{x}_1 + (t_1 - t')\mathbf{x}_2}{t_1 + t_2 - 2t'} \right)^2 + \frac{(\mathbf{x}_1 - \mathbf{x}_2)^2}{(t_1 + t_2 - 2t')}.\quad (\text{A8})$$

The integral over $d^d \mathbf{x}$ is a d -dimensional Gaussian integral, we obtain

$$\langle \delta T_A(\mathbf{x}_1, t_1) \delta T_A(\mathbf{x}_2, t_2) \rangle_c = \frac{\lambda h_0^2}{(4\pi\alpha)^{\frac{d}{2}} \rho^2 c_P^2} \int_{t_0}^{\min(t_1, t_2)} dt' \frac{\exp\left[-\frac{(\mathbf{x}_1 - \mathbf{x}_2)^2}{4\alpha(t_1 + t_2 - 2t')}\right]}{(t_1 + t_2 - 2t')^{\frac{d}{2}}}, \quad (\text{A9})$$

the change of variable $s \equiv (\mathbf{x}_1 - \mathbf{x}_2)^2 / 4\alpha(t_1 + t_2 - 2t')$ gives

$$\begin{aligned} \langle \delta T_A(\mathbf{x}_1, t_1) \delta T_A(\mathbf{x}_2, t_2) \rangle_c &= \frac{\lambda h_0^2}{2(4\pi\alpha)^{\frac{d}{2}} \rho^2 c_P^2} \left[\frac{(\mathbf{x}_1 - \mathbf{x}_2)^2}{4\alpha} \right]^{1-\frac{d}{2}} \int_{\frac{(\mathbf{x}_1 - \mathbf{x}_2)^2}{4\alpha(t_1 + t_2 - 2t_0)}}^{\frac{(\mathbf{x}_1 - \mathbf{x}_2)^2}{4\alpha|t_1 - t_2|}} ds s^{\frac{d}{2}-2} e^{-s} \\ &= \frac{\lambda h_0^2}{2(4\pi\alpha)^{\frac{d}{2}} \rho^2 c_P^2} \left[\frac{(\mathbf{x}_1 - \mathbf{x}_2)^2}{4\alpha} \right]^{1-\frac{d}{2}} \left[\gamma\left(\frac{d}{2} - 1, \frac{(\mathbf{x}_1 - \mathbf{x}_2)^2}{4\alpha|t_1 - t_2|}\right) - \gamma\left(\frac{d}{2} - 1, \frac{(\mathbf{x}_1 - \mathbf{x}_2)^2}{4\alpha(t_1 - t_0 + t_2 - t_0)}\right) \right], \end{aligned} \quad (\text{A10})$$

where $\gamma(s, x)$ is the lower incomplete gamma function. In three spatial dimensions, we obtain

$$\langle \delta T_A(\mathbf{x}_1, t_1) \delta T_A(\mathbf{x}_2, t_2) \rangle_c = \frac{\lambda h_0^2}{8\pi\alpha\rho^2 c_P^2 |\mathbf{x}_1 - \mathbf{x}_2|} \left[\text{Erf}\left(\frac{|\mathbf{x}_1 - \mathbf{x}_2|}{2\sqrt{\alpha|t_1 - t_2|}}\right) - \text{Erf}\left(\frac{|\mathbf{x}_1 - \mathbf{x}_2|}{2\sqrt{\alpha(t_1 + t_2 - 2t_0)}}\right) \right], \quad (\text{A11})$$

using that $\gamma(1/2, x) = \sqrt{\pi} \text{Erf}(\sqrt{x})$.

APPENDIX B: POWER SPECTRA OF ACTIVE FLUCTUATIONS

In d -spatial dimensions, the two-point cumulant $\langle \delta \hat{T}_A(\mathbf{x}_1, \omega_1) \delta \hat{T}_A(\mathbf{x}_2, \omega_2) \rangle_c$ is obtained by taking the Fourier transform of Eq. (27) into real space, which gives

$$\langle \delta \hat{T}_A(\mathbf{x}_1, \omega_1) \delta \hat{T}_A(\mathbf{x}_2, \omega_2) \rangle_c = \lambda \left(\frac{h_0}{\alpha \rho c_P} \right)^2 (2\pi) \delta(\omega_1 + \omega_2) \int \frac{d^d q}{(2\pi)^d} \frac{e^{iq \cdot |\mathbf{x}_1 - \mathbf{x}_2|}}{q^4 + \left(\frac{\omega_1}{\alpha}\right)^2}. \quad (\text{B1})$$

The spectral density is then defined as

$$S_A(|\mathbf{x}|, \omega) \equiv \lambda \left(\frac{h_0}{\alpha \rho c_P} \right)^2 \int \frac{d^d q}{(2\pi)^d} \frac{e^{iq \cdot |\mathbf{x}|}}{q^4 + \left(\frac{\omega}{\alpha}\right)^2}. \quad (\text{B2})$$

For spatial dimension $d = 3, 2, 1$ we obtain for spectral densities

$$S_A(|\mathbf{x}|, \omega)|_{d=3} = \lambda \left(\frac{h_0}{\alpha \rho c_P} \right)^2 \left(\frac{\omega}{\alpha} \right)^{-\frac{1}{2}} \frac{1}{4\sqrt{2}\pi} \frac{\sin \sqrt{\frac{\omega|\mathbf{x}|^2}{2\alpha}}}{\sqrt{\frac{\omega|\mathbf{x}|^2}{2\alpha}}} e^{-\sqrt{\frac{\omega|\mathbf{x}|^2}{2\alpha}}}, \quad (\text{B3})$$

$$S_A(|\mathbf{x}|, \omega)|_{d=2} = -\lambda \left(\frac{h_0}{\alpha \rho c_P} \right)^2 \left(\frac{\omega}{\alpha} \right)^{-1} \frac{1}{2\pi} \text{kei} \sqrt{\frac{\omega|\mathbf{x}|^2}{\alpha}}, \quad (\text{B4})$$

$$S_A(|\mathbf{x}|, \omega)|_{d=1} = \lambda \left(\frac{h_0}{\alpha \rho c_P} \right)^2 \left(\frac{\omega}{\alpha} \right)^{-\frac{3}{2}} \frac{1}{2\sqrt{2}} e^{-\sqrt{\frac{\omega|\mathbf{x}|^2}{2\alpha}}} \left[\sin \sqrt{\frac{\omega|\mathbf{x}|^2}{2\alpha}} + \cos \sqrt{\frac{\omega|\mathbf{x}|^2}{2\alpha}} \right], \quad (\text{B5})$$

where kei is the Kelvin function. In the limit of small frequencies $\omega \ll 2\alpha/|\mathbf{x}|^2$, the spectral density has the scaling behavior

$$S_A(\mathbf{x}, \omega) = C_d \lambda \left(\frac{h_0}{\alpha \rho c_P} \right)^2 \left(\frac{\omega}{\alpha} \right)^{\frac{d}{2}-2}, \quad (\text{B6})$$

where the constant C_d equals $(4\sqrt{2}\pi)^{-1}$, $-\text{kei}(0)(2\pi)^{-1}$ or $(2\sqrt{2})^{-1}$ for $d = 3, 2, 1$, respectively.

APPENDIX C: ACTIVE PART OF THE EFFECTIVE DIFFUSION COEFFICIENT

The effective diffusion coefficient in Eq. (39) is expressed using Eq. (36) as

$$\begin{aligned} D &= \frac{1}{3} \int_0^\infty dt \left\langle \frac{d\mathbf{X}(t)}{dt} \cdot \frac{d\mathbf{X}(0)}{dt} \right\rangle \\ &= \frac{1}{3} \int_0^\infty dt \langle [D_T \nabla T(\mathbf{X}, t) + \boldsymbol{\eta}_X(t)] \cdot [D_T \nabla T(\mathbf{X}, 0) + \boldsymbol{\eta}_X(0)] \rangle \\ &= \frac{D_T^2}{3} \int_0^\infty dt \langle \nabla T(\mathbf{X}, t) \cdot \nabla T(\mathbf{X}, 0) \rangle + \frac{1}{3} \int_0^\infty dt \langle \boldsymbol{\eta}_X(t) \cdot \boldsymbol{\eta}_X(0) \rangle \end{aligned}$$

$$= \frac{D_T^2}{3} \int_0^\infty dt \langle \nabla T(\mathbf{X}, t) \cdot \nabla T(\mathbf{X}, 0) \rangle + D_0, \quad (\text{C1})$$

using that the noise $\eta_{\mathbf{X}}$ and the temperature fluctuations are uncorrelated, which follows from Eq. (36). We have also used the variance of the noise in Eq. (37) to recover D_0 in the last step. The active part of the effective diffusion coefficient is given by

$$\begin{aligned} D_{\text{act}} &= D - D_0 \\ &= \frac{D_T^2}{3} \int_0^\infty dt \langle \nabla T(\mathbf{X}, t) \cdot \nabla T(\mathbf{X}, 0) \rangle \\ &= \frac{D_T^2}{3V} \int_0^\infty dt \left\langle \int \frac{d^3 \mathbf{q}}{(2\pi)^3} q^2 e^{-i\mathbf{q} \cdot [\mathbf{X}(t) - \mathbf{X}(0)]} \delta T_A(\mathbf{q}, t) \delta T_A(-\mathbf{q}, 0) \right\rangle \\ &\simeq \frac{D_T^2}{3V} \int_0^\infty dt \int \frac{d^3 \mathbf{q}}{(2\pi)^3} q^2 \langle e^{-i\mathbf{q} \cdot [\mathbf{X}(t) - \mathbf{X}(0)]} \rangle \langle \delta T_A(\mathbf{q}, t) \delta T_A(-\mathbf{q}, 0) \rangle \\ &\simeq \frac{D_T^2}{3V} \int_0^\infty dt \int \frac{d^3 \mathbf{q}}{(2\pi)^3} q^2 e^{-Dq^2 t} \langle \delta T_A(\mathbf{q}, t) \delta T_A(-\mathbf{q}, 0) \rangle, \end{aligned} \quad (\text{C2})$$

where we have performed a Fourier transform into momentum space in the second step, neglected the correlation between the temperature and the motion in the third step, and finally used the Gaussian approximation

$$\langle e^{-i\mathbf{q} \cdot [\mathbf{X}(t) - \mathbf{X}(0)]} \rangle = e^{-Dq^2 t}. \quad (\text{C3})$$

The correlation function of the active temperature fluctuation in momentum space is given by

$$\langle \delta T_A(\mathbf{q}_1, t_1) \delta T_A(\mathbf{q}_2, t_2) \rangle = \frac{\lambda}{2\alpha} \left(\frac{h_0}{\rho c_P} \right)^2 \frac{e^{-\alpha q_1^2 |t_1 - t_2|}}{q_1^2} (2\pi)^3 \delta^3(\mathbf{q}_1 + \mathbf{q}_2), \quad (\text{C4})$$

which is the Fourier transform of

$$\langle \delta T_A(\mathbf{q}_1, \omega_1) \delta T_A(\mathbf{q}_2, \omega_2) \rangle = \lambda \left(\frac{h_0}{\rho c_P} \right)^2 (2\pi)^4 \frac{\delta^3(\mathbf{q}_1 + \mathbf{q}_2) \delta(\omega_1 + \omega_2)}{(\alpha q_1^2 - i\omega_1)(\alpha q_2^2 - i\omega_2)}, \quad (\text{C5})$$

with respect to ω_1 and ω_2 . Substituting Eq. (C4) into Eq. (C2) and using that $(2\pi)^3 \delta^3(\mathbf{q} = 0) = V$, we obtain

$$\begin{aligned} D_{\text{act}} &= \frac{\lambda D_T^2}{6\alpha} \left(\frac{h_0}{\rho c_P} \right)^2 \int_0^\infty dt \int \frac{d^3 \mathbf{q}}{(2\pi)^3} e^{-(D+\alpha)q^2 t} \\ &= \frac{\lambda D_T^2}{6\alpha} \left(\frac{h_0}{\rho c_P} \right)^2 \frac{1}{D+\alpha} \int \frac{d^3 \mathbf{q}}{(2\pi)^3} \frac{1}{q^2} \\ &= \frac{\lambda D_T^2}{6\alpha} \left(\frac{h_0}{\rho c_P} \right)^2 \frac{1}{D+\alpha} \frac{1}{2\pi^2} \int_0^{2\pi/a} dq \\ &= \frac{\lambda D_T^2}{6\pi\alpha a} \left(\frac{h_0}{\rho c_P} \right)^2 \frac{1}{(D+\alpha)}, \end{aligned} \quad (\text{C6})$$

where we have introduced a cut-off for large q , namely $2\pi/a$ where a is the size of the tracer particle.

From Eq. (C6) and using that $D_T = S_T D_0$ and $D = D_0 + D_{\text{act}}$, the ratio D_{act}/D_0 is given by the quadratic polynomial

$$\left(\frac{D_{\text{act}}}{D_0} \right)^2 + \left(\frac{D_{\text{act}}}{D_0} \right) \left(1 + \frac{\alpha}{D_0} \right) - C = 0, \quad (\text{C7})$$

where the dimensionless coefficient C is defined in Eq. (43). The solution of Eq. (C7) is

$$\left(\frac{D_{\text{act}}}{D_0} \right) = -\frac{1}{2} \left(1 + \frac{\alpha}{D_0} \right) \pm \frac{1}{2} \sqrt{\left(1 + \frac{\alpha}{D_0} \right)^2 + 4C}. \quad (\text{C8})$$

In absence of activity, corresponding to $\lambda = 0$ and therefore $C = 0$, D_{act} vanishes. Considering the two solutions of Eq. (C8) in the limit of vanishing C allows the identification of the solution with a positive sign as the physical one.

The Soret coefficient for which $D_{\text{act}} = D_0$ is obtained from Eqs. (43) and (44) as

$$S_{T,\text{co}}(a) = \left(\frac{\rho c_P}{h_0} \right) \sqrt{\frac{6\pi\alpha a}{\lambda} \left[\frac{6\pi\eta\alpha a}{k_B T} + 2 \right]}, \quad (\text{C9})$$

having expressed the passive diffusion coefficient as $D_0 = k_B T / (6\pi\eta a)$, where η is the viscosity. The crossover coefficient $S_{T,co}$ is a monotonically increasing function of the particle size a . For values of the Soret coefficient smaller than $S_{T,co}$, the fluctuations of the concentration are well described by local-equilibrium thermodynamics. For the parameters associated with the living cells, the viscosity water,

and tracer particle size a of the order 10^{-9} m, we have $S_{T,co} \sim 10^9 \text{ K}^{-1}$, which is larger than typical values reported in the literature ($S_T \sim 10^{-5} - 10^{-3} \text{ K}^{-1}$ in Ref. [46] and $S_T \sim 10^{-2} - 10^2 \text{ K}^{-1}$ in Ref. [40]) supporting the result that the concentration fluctuations do not break the local equilibrium hypothesis for the spatiotemporal scales identified previously.

- [1] M. C. Marchetti, J.-F. Joanny, S. Ramaswamy, T. B. Liverpool, J. Prost, M. Rao, and R. A. Simha, Hydrodynamics of soft active matter, *Rev. Mod. Phys.* **85**, 1143 (2013).
- [2] F. Jülicher, A. Ajdari, and J. Prost, Modeling molecular motors, *Rev. Mod. Phys.* **69**, 1269 (1997).
- [3] J. Prost, F. Jülicher, and J.-F. Joanny, Active gel physics, *Nat. Phys.* **11**, 111 (2015).
- [4] C. A. Weber, D. Zwicker, F. Jülicher, and C. F. Lee, Physics of active emulsions, *Rep. Prog. Phys.* **82**, 064601 (2019).
- [5] B. Alberts, D. Bray, K. Hopkin, A. D. Johnson, J. Lewis, M. Raff, K. Roberts, and P. Walter, *Essential Cell Biology* (Garland Publishing, New York, NY, 2013).
- [6] J. Howard, *Mechanics of Motor Proteins and the Cytoskeleton* (Sinauer Associates, New York, NY, 2001).
- [7] P. Nelson, *Biological Physics* (W. H. Freeman, New York, NY, 2004).
- [8] T. R. Kießling, R. Stange, J. A. Käs, and A. W. Fritsch, Rheology of living cells—Impact of temperature variations on cell mechanics, *New J. Phys.* **15**, 045026 (2013).
- [9] D. Chrétien, P. Bénit, H.-H. Ha, S. Keipert, R. El-Khoury, Y.-T. Chang, M. Jastroch, H. T. Jacobs, P. Rustin, and M. Rak, Mitochondria are physiologically maintained at close to 50°C , *PLoS Biol.* **16**, e2003992 (2018).
- [10] S. Sotoma, C. Zhong, J. C. Y. Kah, H. Yamashita, T. Plakhotnik, Y. Harada, and M. Suzuki, In situ measurements of intracellular thermal conductivity using heater-thermometer hybrid diamond nanosensors, *Sci. Adv.* **7**, eabd7888 (2021).
- [11] P. Song, H. Gao, Z. Gao, J. Liu, R. Zhang, B. Kang, J.-J. Xu, and H.-Y. Chen, Heat transfer and thermoregulation within single cells revealed by transient plasmonic imaging, *Chem* **7**, 1569 (2021).
- [12] C. P. Brangwynne, C. R. Eckmann, D. S. Courson, A. Rybarska, C. Hoegge, J. Ghazkhani, F. Jülicher, and A. A. Hyman, Germline P granules are liquid droplets that localize by controlled dissolution/condensation, *Science* **324**, 1729 (2009).
- [13] P. Li *et al.*, Phase transitions in the assembly of multivalent signalling proteins, *Nature (London)* **483**, 336 (2012).
- [14] A. W. Fritsch, A. F. Diaz-Delgado, O. Adame-Arana, C. Hoegge, M. Mittasch, M. Kreysing, M. Leaver, A. A. Hyman, F. Jülicher, and C. A. Weber, Local thermodynamics governs the formation and dissolution of protein condensates in living cells, *Proc. Natl. Acad. Sci. USA* **118**, e2102772118 (2021).
- [15] A. A. Hyman, C. A. Weber, and F. Jülicher, Liquid-liquid phase separation in biology, *Annu. Rev. Cell Dev. Biol.* **30**, 39 (2014).
- [16] R. P. Feynman and A. R. Hibbs, *Quantum Mechanics and Path Integrals* (McGraw Hill, New York, NY, 1965).
- [17] P. Hänggi, On derivations and solutions of master equations and asymptotic representations, *Z. Phys. B* **30**, 85 (1978).
- [18] P. Hänggi, Correlation functions and master equations of generalized non-Markovian Langevin equations, *Z. Phys. B* **31**, 407 (1978).
- [19] P. Hänggi, Langevin description of Markovian integro-differential master equations, *Z. Phys. B* **36**, 271 (1980).
- [20] N. G. van Kampen, in *Thermodynamics and Kinetics of Biological Systems*, edited by I. Lamprecht and A. I. Zotin (De Gruyter, Berlin, 1983).
- [21] N. G. van Kampen, *Stochastic Processes in Physics and Chemistry* (Elsevier, Amsterdam, 1992).
- [22] J. Zinn-Justin, *Quantum Field Theory and Critical Phenomena* (Clarendon Press, Oxford, UK, 2002).
- [23] L. D. Landau and E. M. Lifshitz, *Course of Theoretical Physics: Fluid Mechanics* (Pergamon Press, Oxford, UK, 1987), 2nd ed.
- [24] M. N. Ozisic, *Heat Conduction* (John Wiley and Sons, New York, NY, 1993).
- [25] L. D. Landau and E. M. Lifshitz, *Statistical Physics, Part 1* (Pergamon Press, Oxford, UK, 1985), 3rd ed.
- [26] L. D. Landau, E. M. Lifshitz, and L. P. Pitaevskii, *Course of Theoretical Physics: Statistical Physics, Part 2* (Pergamon Press, Oxford, UK, 1981), 2nd ed.
- [27] D. Forster, *Hydrodynamic Fluctuations, Broken Symmetry, and Correlation Functions* (W. A. Benjamin, Advanced Book Program, Menlo Park, CA, 1975).
- [28] H. Frisken and T. Frank, *The Fokker-Planck Equation* (Springer-Verlag, Berlin, 1996).
- [29] R. F. Voss and J. Clarke, Flicker (1/f) noise: Equilibrium temperature and resistance fluctuations, *Phys. Rev. B* **13**, 556 (1976).
- [30] M. S. Schlesinger, Fractal time and 1/f noise in complex systems, *Ann. N.Y. Acad. Sci.* **504**, 214 (1987).
- [31] L. Wentian, Spatial 1/f spectra in open dynamical systems, *Europhys. Lett.* **10**, 395 (1989).
- [32] P. Szendro, G. Vincze, and A. Szasz, Pink-noise behaviour of biosystems, *Eur. Biophys. J.* **30**, 227 (2001).
- [33] A. R. Butz, A theory of 1/f noise, *J. Stat. Phys.* **4**, 199 (1972).
- [34] R. M. Corless, G. H. Gonnet, D. E. G. Hare, D. J. Jeffrey, and D. E. Knuth, On the Lambert W function, *Adv. Comput. Math.* **5**, 329 (1996).
- [35] What is the power consumption of a cell? book.bionumbers.org/what-is-the-power-consumption-of-a-cell/. Accessed 20 January 2022.
- [36] A. Thommen *et al.*, Body size-dependent energy storage causes Kleiber's law scaling of the metabolic rate in planarians, *eLife* **8**, e38187 (2019).
- [37] J. Blumm and A. Lindemann, Characterization of the thermophysical properties of molten polymers and liquids using the flash technique, *High Temp. High Press.* **35/36**, 627 (2003).

- [38] H. Spohn, *Large Scale Dynamics of Interacting Particles* (Springer-Verlag, Berlin, 1991).
- [39] A. Basu, J.-F. Joanny, F. Jülicher, and J. Prost, Anomalous behavior of the diffusion coefficient in thin active films, *New J. Phys.* **14**, 115001 (2012).
- [40] S. Duhr, and D. Braun, Why molecules move along a temperature gradient, *Proc. Natl. Acad. Sci. USA* **103**, 19678 (2006).
- [41] P. Martin, A. J. Hudspeth, and F. Jülicher, Comparison of a hair bundle's spontaneous oscillations with its response to mechanical stimulation reveals the underlying active process, *Proc. Natl. Acad. Sci. USA* **98**, 14380 (2001).
- [42] A. J. Levine, and F. C. MacKintosh, The mechanics and fluctuation spectrum of active gels, *J. Phys. Chem. B* **113**, 3820 (2009).
- [43] C. Riedel, R. Gabizon, C. A. M. Wilson, K. Hamadani, K. Tsekouras, S. Marqusee, S. Pressé, and C. Bustamante, The heat released during catalytic turnover enhances the diffusion of an enzyme, *Nature (London)* **517**, 227 (2015).
- [44] R. Golestanian, Enhanced Diffusion of Enzymes that Catalyze Exothermic Reactions, *Phys. Rev. Lett.* **115**, 108102 (2015).
- [45] J. Agudo-Canalejo, P. Illien, and R. Golestanian, Cooperatively enhanced reactivity and “stabilitaxis” of dissociating oligomeric proteins, *Proc. Natl. Acad. Sci. USA* **117**, 11894 (2020).
- [46] S. R. de Groot and P. Mazur, *Nonequilibrium Thermodynamics* (Dover, New York, NY, 1984).